

1 SMASH: Spitzer Merger History and Shape of the Galactic Halo

Cold Dark Matter (CDM) models of the universe predict a hierarchical assembly of structures. In particular, they show that galaxies like the Milky Way (MW) build up over time by a series of mergers of other CDM halos and their attendant populations of baryonic stars and gas. These are discrete events with orbits being determined by a combination of cosmological infall and local interactions of halo mass distributions. Each event is a unique tracer of cosmological evolution in the near universe.

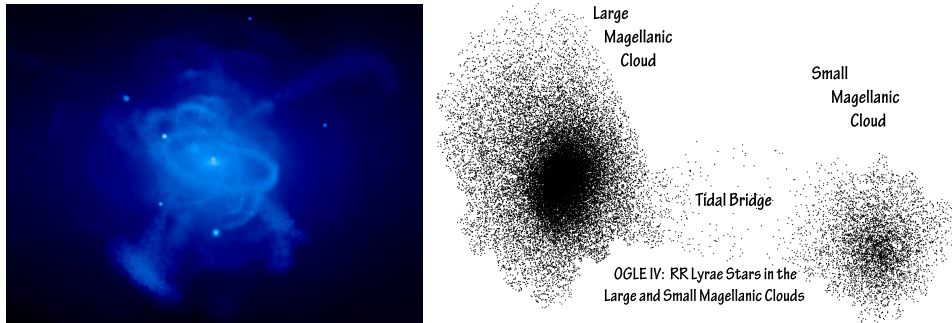


Figure 1 Left: CDM simulation of satellite accretion onto a dark-matter halo, similar to that of the MW (Bullock & Johnston 2005, ApJ, 635, 931). Right: Distribution of RR Lyrae stars from the LMC (left) across the bridge to the SMC (right) (OGLE IV pre-release data showing the first detection of RR Lyrae variables in the bridge region connecting the two interacting satellites).

The instantaneous kinematics and three-dimensional distribution of stars and gas found in the extended halos, streams and tidal tails surrounding companion galaxies to the MW encode the time evolution of their decaying orbits. These orbits in turn reflect the external constraints imposed upon them by the total (dark and baryonic) mass distribution of the MW itself. By studying the orbits of satellites to the MW, currently in different phases of merging, we can illuminate not only the histories of these individual sub-systems but also shed light on the structure of the galaxy itself, and probe the time evolution and merger history of the MW as a hierarchical system. The targets are the Large/Small Magellanic Cloud (LMC/SMC) system on its first pass through the MW halo, the merger of the Sagittarius dwarf, well underway within the MW, and 3 more distant satellites.

When it was planned and then launched, Spitzer was never thought to be a satellite that would make fundamental contributions to the 3D structure of the Milky Way or its local environs. However, in its Warm Mission, Spitzer has totally revolutionized our ability to determine high-precision distances within and beyond our own galaxy. The first breakthrough came with the reconstruction of the extragalactic distance scale using the mid-IR period-luminosity relation for Population I Cepheid variables (Freedman et al. 2011, AJ, 142, 192). We now have the equally exciting opportunity of using the ultra-precise, mid-IR PL relation for RR Lyrae stars, whose zero point was calibrated by HST just last year. This new path opens up a wide range of novel and important science applications. The “*Spitzer Merger History and Shape of the Galactic Halo*” (SMASH) program will use RR Lyrae variables to make the most precise determination of the 3D structure of on-going merger and tidal disruption events within and around the Milky Way. In a complementary program, the *Carnegie RR Lyrae Program* will establish the absolute calibration of the RR Lyrae PL relation in the two IRAC bands (3.6 and 4.5 μm) being used here.

1.1 Synergies and Strengths

This particular program has very specific science goals that are uniquely enabled by Spitzer, but it is also very tightly coupled with both a parallel proposal, the Carnegie RR Lyrae Program (CRRP), and several on-going ground-based surveys (OGLE IV & VMC). In addition it is laying the foundations for other important science that will be enabled by a combination of the Spitzer distances with Gaia proper motions. To this end our team is a cooperative effort, made up of lead scientists and principal investigators from OGLE (Udalski [PI], Pietrzynski & Soszynski), from the *Vista Survey of the Magellanic System : VMC* (Maria-Rosa Cioni [PI]), and from Gaia (Clementini). We are provisionally reliant on the zero-point calibration of the RR Lyrae PL relation coming from the CRRP; however, if that program does not get scheduled we are prepared to reprogram some of our time to obtain mean magnitudes and derive absolute magnitudes for the four RR Lyrae variables that currently have HST parallaxes, setting the zero point for the RR Lyrae PL relation.

The CRRP proposal documents and justifies the enormous advantages offered by Spitzer in using the mid-IR PL relation for RR Lyrae variables. We will not repeat those arguments here, but simply state a few of the high-level reasons for undertaking these programs using Spitzer in combination with decades of foundational work that has been executed from the ground. First and foremost, all of the variable stars being targeted by Spitzer are already known; they have precise positions, accurate periods, well-defined light curves, and phases that will be up-dated in real time with the Spitzer observations through on-going ground-based monitoring. Reddening is a major systematic that must be addressed in all of the interpretive studies using RR Lyrae stars as probes of distances. Because of the monotonically declining extinction as a function of increasing wavelength the Spitzer data will be at least 5 times less affected by reddening than any existing ground-based data. Metallicity is the major (and still controversial) contributor to scatter in the **optical** PL relations for RR Lyrae stars; its effects are so diminished in the infrared that they have yet to be detected at those wavelengths (although the CRRP will test for them). Finally, the RR Lyrae IRAC PL relation has a precision of $\pm 2\%$, unequalled by any other known stellar distance indicator. The convergence of all of these factors puts Spitzer in a unique position to rapidly address and definitively answer questions that could not have been considered possible to pose, even just one year ago.

1.2 Summary of Science Goals

- A survey of the exact form and 3-dimensional structure of the halo surrounding the Large Magellanic Cloud [Section 2]
 - High-precision and systematically accurate distances to the individual LMC/SMC satellites of the Milky Way [Sections 2 & 3]
 - 3D maps of the structure of the interaction bridge and tail between the LMC and the disrupted Small Magellanic Cloud [Section 3]
 - A refined interpretation of microlensing events towards the Large Magellanic Cloud given the RR Lyrae-mapped structure of the LMC halo [Section 4]
 - A determination of the distance and a delineation of the 3-dimensional structure of the core and debris tail of the Milky Way-merging Sagittarius Dwarf galaxy [Section 5]
 - Improved constraints on the radial profile and shape of the Milky Way’s CDM halo. [Section 5.2]
 - Precise determinations of the distances to three of the closest dwarf galaxies demonstrably interacting with the Milky Way. [Section 6]
 - A zero-point of the Tip of the Red Giant Branch Method using TRGB stars in the halo of the LMC calibrated by the co-spatial RR Lyrae population [Section 6.1]

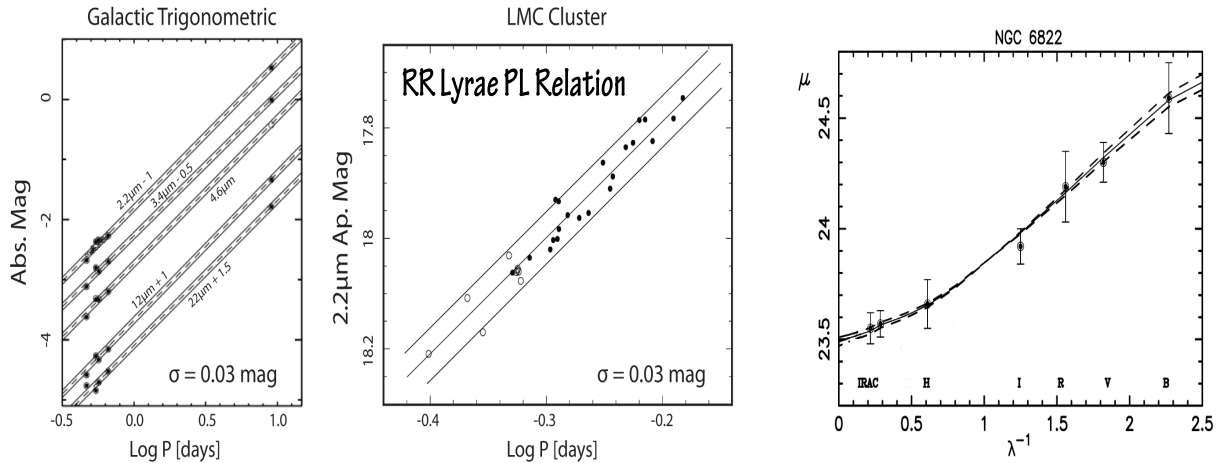


Figure 2 Infrared PL relations for RR Lyrae variables. **Left Panel:** The four Galactic RR Lyrae variables and the one W Virginis star observed by Benedict et al. (2011, AJ, 142, 1871) using HST to determine absolute trigonometric parallaxes. The $3.4 - 22 \mu\text{m}$ observations are from WISE. **Middle Panel:** The observed $2.2 \mu\text{m}$ portion of the $2.2 \mu\text{m}$ PL relation for RR Lyrae stars in the LMC globular cluster, Reticulum (Dall’Ora et al. 2004, ApJ, 610, 269). Open circles are overtone (RRc) pulsators, corrected to their fundamental period. Filled circles are fundamental (RRab) pulsators. At all 5 wavelengths the scatter around the mean relation is only ± 0.03 mag (for Cepheids the scatter about their mid-IR PL relation is ± 0.11 mag); and the slopes of the LMC and Galactic samples in the near-infrared are indistinguishable. Flanking lines are all $\pm 2\sigma$. **Right Panel:** An example of the multi-wavelength fitting technique for simultaneously deriving extinctions (slope of the fit) and true moduli (long-wavelength intercept) leveraging optical, near-infrared and Spitzer/IRAC mid-IR observations. Adapted from Madore et al. 2009, ApJ, 693, 936 for Cepheids in NGC 6822. The same technique will be used for individual RR Lyrae variables to be observed in this program, yielding reddening-corrected distances individually good to $\pm 2\%$.

2 3D Structure of the LMC: Disk, Bar, and Halo

Kinematical observations for the LMC have been obtained using many tracers. The kinematics of gas in the LMC has been studied primarily using HI (e.g., Kim et al. 1998, ApJ, 503, 674; Olsen & Massey 2007). Discrete LMC tracers which have been studied kinematically include star clusters, planetary nebulae, HII regions, red supergiants, red giant branch (RGB) stars (Zhao et al. 2003, MNRAS, 339, 701; Cole et al. 2005, AJ, 129, 1465), carbon stars and RR Lyrae stars (e.g., Minniti et al. 2003, Science, 301, 1508; Borissova et al. 2005 and references therein). For the majority of tracers, the line-of-sight velocity dispersion is at least a factor ~ 2 smaller than their rotation velocity. This implies that on the whole the LMC is a (kinematically cold) disk system.

Two angles determine the geometry under which we view the LMC disk: the inclination i and the line-of-nodes position angle Θ . These angles have been estimated using either geometrical or kinematical methods. In geometrical methods ones measures relative distances between tracer populations, combined with the fact that some parts of an inclined disk are closer to the observer than others. In kinematical methods one measures and models the velocity fields of tracers (usually under the assumption of circular orbits). Applications of the geometric method have been based on RGB and AGB stars detected with the 2MASS and DENIS surveys (van der Marel & Cioni 2001, AJ, 122, 1807), Cepheids (Persson et al. 2004, AJ, 128, 2239; Nikolaev et al. 2004, ApJ, 601, 260), or red clump stars (Olsen & Salyk 2002, AJ, 124, 2045). Applications of the kinematical method have been based on the line-of-sight velocities of carbon stars (van der Marel et al. 2002), red-supergiants (Olsen & Massey 2007, ApJ, 656, L610), or HI (Olsen et al. 2011, ApJ, 737, 29); or on the average proper motions of LMC star fields observed with HST (van der Marel & Kallivayalil in prep.).

All studies agree that i is approximately in the range 30° – 40° , whereas Θ appears to be in the range 120° – 150° . However, the variations between the results from different studies significantly exceed the random errors. This may be due to a combination of systematic errors, spatial variations in the viewing angles (e.g., warps and twists of the disk plane; van der Marel & Cioni 2001; Olsen & Salyk 2002; Subramaniam 2003, ApJ, 598, L19; Nikolaev et al. 2004) combined with differences in spatial sampling between studies, contamination by possible out of plane structures, and differences between different tracer populations. **As a result, even the most basic property of the LMC disk, namely its geometry, remains poorly understood. This limits our ability to determine deviations from a flat disk geometry, which are important for understanding the LMC-SMC-MW interaction as well as microlensing statistics.**

The LMC consists of an outer body that appears elliptical in projection on the sky, with a pronounced, off-center bar. The appearance in the optical wavelength regime is dominated by regions of strong star formation, and patchy dust absorption. However, when only RGB and carbon stars are selected from near-IR surveys such as 2MASS, the appearance of the LMC morphology is actually quite regular and smooth (van der Marel 2001). The position angle of the projected major axis of the LMC on the sky ($\text{PA}_{\text{ma},\text{axis}} = 189.3 \pm 1.4^\circ$) differs from the position angle Θ of the line of nodes. This implies that the LMC has an in-plane ellipticity ϵ in the range ~ 0.2 – 0.3 . This is larger than typical for disk galaxies, and is probably due to tidal interactions with either the SMC or the MW.

As in the MW, younger populations have a smaller velocity dispersion, and hence a smaller scale height, than older populations. It has been suggested that the stars with the

highest dispersion (i.e., 50 km/s for RR Lyrae stars from Minniti et al. 2003; Borissova et al. 2006, A&A, 460, 459) may form a halo distribution and not be part of the LMC disk. On the other hand, this remains unclear, since the kinematics of these stars have typically been observed only in the central region of the LMC. Therefore, it is not known whether the rotation properties of this population are consistent with being a separate halo component. In fact, the surface density distribution of the LMC RR Lyrae stars is well fit by an exponential with the same scale length as inferred for other tracers known to reside in the disk (Alves 2004, ApJ, 601, L151). Either way, the vertical extent of all LMC populations is certainly significant.

The LMC bar is a very poorly understood structure. Its center is offset from the dynamical center of HI gas (Kim et al. 1998) and stars by about 1 kpc. Moreover, the bar does not reveal its presence in either the distribution or kinematics of gaseous tracers. Most likely, the bar is a transient feature induced by the interaction with the SMC (e.g., Besla et al. 2012, MNRAS, 421, 2109). Its structure has been the topic of considerable study and debate, and in particular the question of whether or not it resides in the LMC disk plane. The Spitzer RR Lyrae data will have the precision to resolve this very issue.

Nikolaev et al. (2004) studied the relative distances of more than 2000 Cepheids in the central region of the LMC, and argued that the data implied the presence of a symmetric warp in the disk, and that the bar is located about 0.5 kpc in front of the main disk. Interestingly, an offset between the LMC bar and disk had previously been suggested by Zhao & Evans (2000, AJ, 545, L35) as an explanation for the observed LMC microlensing optical depth (see also Olsen & Salyk (2002) and Subramanian 2003). **Quantifying what any exact warping of the disk is, and what any displacement or misalignment of the bar is, would be important for constraining the details of the LMC-SMC-MW interaction.**

Of particular relevance to studies of microlensing results (see Section 4) is the possible presence of foreground or background populations in the LMC area of the sky. It has been suggested that there might be a population of stars in front of or behind the LMC that was pulled from the Magellanic Clouds due to the LMC-SMC-MW interaction (Zhao 1998; Besla et al. 2012). Or there might be a non-virialized shroud of stars at considerable distances above the LMC plane due to MW tidal heating (Weinberg 2000, ApJ, 532, 922; Evans & Kerins 2000, ApJ, 529, 917). However, the recent detection that about 5% of LMC stars have anomalous kinematics, inconsistent with the disk rotation (Olsen et al. 2011), does make it credible that out-of-plane populations exist in the LMC, possibly pulled tidally from the SMC (see Section 3). **Constraining the nature and 3D distribution of these stars is critical for constraining the details of the LMC-SMC-MW interaction, as well-as-their microlensing signature. And quantifying the larger-radius structure of the LMC, whether it has a stellar halo, and what its properties are (e.g., substructure, triaxiality) would be important for constraining hierarchical structure formation models in general, and the LMC-SMC-MW interaction history in particular.**

[40 halo + 20 main body pointings: 220 hr]

3 3D Structure of the Disrupted SMC and Tidal Bridge

The Magellanic Clouds are our closest example of an interacting pair of dwarf galaxies. The interaction is clearly illustrated by the pronounced bridge of HI gas connecting the Large and Small Magellanic Clouds (LMC and SMC), known as the Magellanic Bridge (Kerr 1957, AJ, 62, 93; Putman et al. 2003, ApJ, 586, 170). All theoretical models of the Magellanic System predict that the Magellanic Bridge formed via a recent tidal encounter between the LMC and SMC (e.g., Gardiner & Noguchi 1996, MNRAS, 278, 191). Such an encounter is unavoidable according to the high-precision proper motions from the HST by Kallivayalil et al. (2006, ApJ, 652, 1213); backward orbital integration using the present day proper motion vectors imply that the Clouds were much closer to each other 100-300 Myr ago than their current 20 kpc separation. However, the exact impact parameter of this interaction is unknown, ranging from separations larger than the HI radius of the LMC (10 kpc; all traditional models e.g. Gardiner & Noguchi 1996, MNRAS, 278, 191) to a direct collision (impact parameter < 5 kpc; Besla et al. 2012, MNRAS, 421, 2109). These two extremes have different consequences for the recent star formation histories of these galaxies, their internal kinematics and in particular for their current 3D structure. **The recent interaction history of the Magellanic Clouds will leave indelible marks in the 3D structure of both the LMC and SMC that can be used to constrain the nature of their most recent interaction.**

Quantifying the 3D structure of the LMC’s disk/bar will place significant constraints on the dynamical nature of the LMC’s stellar bar and the impact parameter of the recent LMC-SMC interaction. Although the SMC is classified as an Irregular dwarf galaxy, its older stellar distribution is better described as a spheroidal structure (Zaritsky et al. 2000, ApJ, 534, L53), meaning that its irregular appearance in the optical seems to owe to disorganized, on-going star formation. Furthermore, a dichotomy exists between the HI and stellar kinematics of the SMC. Harris & Zaritsky (2006, AJ, 131, 2514) examined 2,046 RGB stars and found a velocity dispersion of $\sigma = 27.5 \pm 0.5$ km/s with little rotation. The low V_{rot}/σ is consistent with that of dE and dSph galaxies. In sharp contrast, the observed line-of-sight velocity field of the HI reveals a large gradient of 100 km/s across the extent of the SMC (Stanimirovic et al., 2004, ApJ, 604, 176). The distinct HI and stellar kinematics mark the SMC as a potential transition object between a rotationally supported dwarf irregular galaxy and a dispersion supported dwarf spheroidal; however, the mechanism that facilitated this transition is unclear. Only young (O,B,A) stars show signs of rotation, implying that the transition was recent and likely intimately linked with the nature of the LMC-SMC encounter. A direct collision, for example, can shock heat the SMC’s stellar disk, morphologically transforming it to a spheroid (Besla et al. in prep). However, the interpretation of the HI line-of-sight kinematics depends critically on our understanding of the 3D geometry of the SMC: are we looking at the SMC face-on or edge-on?

Despite its proximity to the MW, the geometry of the SMC is poorly understood. The SMC is known to be significantly extended along our line-of-sight (Welch et al. 1987, ApJ, 321, 162; Mathewson et al. 1986, ApJ, 301, 664); the SMC’s main body is consequently often described as a “bar”. The line-of-sight depth increases along the northeastern side of the SMC, which connects to the Magellanic Bridge, suggesting a link to interactions with the LMC (Gardiner & Hatzidimitriou 1992, MNRAS, 257, 195). The exact values of this depth are subject to debate, ranging from 10 to 75 kpc (e.g., Mathewson et al. 1986). The geometry of the SMC’s extended and internal stellar components is critical in the assessment

of the degree to which external influences have shaped its evolution.

We will use individual RR Lyrae star distances to quantify the 3D geometry of the SMC. At the distance of the SMC (60 kpc), our expected random errors of 2% correspond to 1.2 kpc, which is 10-15 times smaller than the expected line-of-sight depth of 8-20 kpc, and at least 3 times more precise than previously attempted mappings using Cepheids or Red Clump stars (e.g., Welch et al., 1987, ApJ, 321, 162).

[30 main body + 10 bridge pointings: 150 hr]

4 Microlensing Events towards the LMC

Paczynski (1986, ApJ, 304, 1) suggested that massive compact halo objects (MACHOs) could be found by monitoring the brightness of several million stars in the Magellanic Clouds in search for microlensing by unseen foreground lenses. There have been a number of surveys conducted towards the MCs in search of microlensing events, such as the MACHO survey (Alcock et al. 2000, ApJ, 542, 281), EROS (Tisserand et al. 2007, A&Ap, 469, 387) and OGLE (Udalski 1997, AcA, 57, 319). The goal of these surveys was to test the hypothesis that MACHOs could be a major component of the dark matter halo of the MW. After 20 years of work, a number of microlensing events were detected towards the LMC by the OGLE and MACHO teams, but a clear explanation for their origin remains elusive. This Spitzer program will shed new light on this problem.

Self-lensing by stars in the LMC's disk (e.g., Saha 1994, Nature, 370, 275) may explain the events detected by the OGLE team (Calchi Novati et al. 2011, MNRAS, 416, 1292). However, attempts to explain the MACHO team's larger number of reported events using a variety of disk and spheroid models for the LMC and MW have failed to explain their reported microlensing optical depth at the 99.9% level (Bennett 2005, ApJ, 633, 906). Alternatively, stellar debris stripped from the SMC or previously accreted satellites that form the stellar halo of the LMC, may provide a natural explanation for the reported microlensing events (Besla et al. 2012, ArXiv 1205.4724; Zhao (1998, MNRAS, 294, 139)).

By understanding the 3D geometry of the LMC stellar halo (Section 2) and interaction history with the SMC (Section 3) we can better constrain the distribution of the stellar debris that may be acting as the sources or lensing population for the microlensing signal observed towards the LMC by the MACHO survey.

5 The Sagittarius Dwarf Spheroidal Galaxy

The Sagittarius Dwarf Galaxy (hereafter Sgr) was discovered serendipitously during a radial velocity survey of the Galactic bulge (Ibata et al. 1994, Nature, 370, 194). While the number of known MW satellites has more than doubled recently (e.g., McConnachie, 2012, AJ, 144, 4), in many ways Sgr remains the most studied and most intriguing — it is the closest satellite, among the largest (only the LMC and SMC are more luminous), and has the most prominent stellar tidal tails.

From the first maps of the Sgr core (Ibata et al. 1994; Ibata et al. 1995, MNRAS, 277, 781) its elongated morphology suggested destruction by tidal forces, as might be anticipated from its proximity to the Galaxy. Subsequent N-body models confirmed the validity of this interpretation (Velazquez & White, 1995, MNRAS, 275, L23) and showed that debris from

Sgr should form coherent streams of stars encircling our Galaxy (Johnston et al. 1995, ApJ, 451, 598). Signatures of these giant star streams have since been discovered in many studies, and comprehensively mapped across the sky in carbon stars (Totten & Irwin, 1998, MNRAS, 294, 1) M giant stars selected from the Two Micron All Sky Survey (Majewski et al. 2003, ApJ, 599, 1082) and main sequence turnoff stars selected from the Sloan Digital Sky Survey (Belokurov et al. 2006, ApJ Lett, 642, L137). Distance estimates along the tail have been derived from these photometric surveys (e.g., Martínez-Delgado et al. 2004, ApJ, 601, 241) and gradients in radial velocities and stellar populations measured with follow-up spectroscopy (e.g., Keller et al. 2010, ApJ, 720, 940). These rich data sets have inspired equally rich interpretations of Sgr debris (e.g., Law & Majewski, 2010, ApJ, 714, 229 – hereafter LM10). Figure 3 (left panel) illustrates typical results from an N-body simulation of dwarf satellite disruption along the expected Sgr orbit, with particles projected onto the plane perpendicular to the Galactic disk containing both the Sun and Galactic center.

LM10 demonstrate how a comparison of N-body simulations with the observed debris enables a detailed reconstruction of Sgr’s history — its mass and stellar content, orbit, rate of destruction and even original distribution in populations. Moreover, the phase-space distribution of the debris offers a unique probe of the depth, shape and extent of the Milky Way’s dark matter halo that cannot be matched using other techniques on our own or other galaxies (e.g., Ibata et al. 2001, ApJ, 551, 294). Most recently, LM10 have combined all current data on Sgr debris to assess the triaxiality and orientation of the outer Galaxy — the first time that such a reconstruction of the 3-dimensional mass distribution of a dark matter halo has been feasible. These constraints on Sgr’s mass and orbit have invigorated discussions of Sgr in a more cosmological context, the mass and extent of the original dark matter halo that hosted it as well as its effect on the MW itself (e.g., Michel-Dansac et al. 2011, MNRAS, 414, L1). We propose to use Spitzer to measure accurate distances to both Sgr and its debris, significantly advancing our understanding of Sgr and its interaction with the MW, as well as the nature of its progenitor and the shape of the Galactic potential.

5.1 Probing the Sagittarius Core by Its Prominent RR Lyrae Population

We will target 21 fields within the core of the Sgr dSph, including (a) a pointing centered on the globular cluster M54, situated at the Sgr center, (b) another 8 “pure Sgr” core fields in a 1 deg radius ring encircling, but excluding, M54, and (c) two groups of six pointings flanking either side of Sgr center along the major axis at the 220 arcmin ($= 1.9$ kpc) half light radius ($r_{1/2}$). Almost all of the 194 known M54 RR Lyrae (Montiel & Michell, 2010, AJ, 140, 1500) will fit within a single IRAC pointing (while perhaps a quarter of these will be lost to crowding). Exact positioning of the “pure Sgr” fields will be optimized to yield 2-3 Sgr RR Lyrae each (Sgr’s central RRab Lyrae density is 139 deg^{-2} ; Cseresnjes, 2001, A&Ap, 375, 909), while each of the dozen flanking fields will have 1-2 RR Lyrae each, so that, in total, we expect of order (a) 100 RR Lyrae from M54, (b) 20 RR Lyrae from the Sgr center ring, and (c) 7 more Sgr RR Lyrae in each of the flanking regions. A 2% distance precision per Sgr RR Lyrae (~ 30 kpc) requires 30 min integrations per visit; a dozen visits to each of the 21 fields thus totals 126 hours. These data will serve to answer several key questions about the Sgr system:

- **Three-Dimensional Shape and Orientation of the Core:** Sgr is the most elliptical of the Milky Way satellites (axis ratio $B/A = 0.53$ within $2r_{1/2}$; Majewski et al. 2003, ApJ, 599, 1082; Lokas et al. 2012, ApJ, 751, 61) and the origin of this ellipticity is unclear. The true three-dimensional shape of the system might be prolate (i.e., bar-like), but it could also be oblate with the minor axis in the plane of the sky. The shape is relevant to the dynamical state of the system: An oblate system would favor models postulating that Sgr progenitor is a disk galaxy (Peñarrubia et al. 2010, MNRAS, 408, L26) whereas establishing that Sgr is currently prolate would, e.g., fit the evolutionary scenario proposed by Lokas et al. (2010, ApJ, 725, 1516) wherein the system has been transformed into a bar-like morphology via “tidal stirring” of an initial disk. While lack of clear Sgr rotation disfavors the Sgr disk hypothesis (Peñarrubia, et al. 2011, ApJL, 727, L2; Frinchaboy et al. 2012, ApJ, in press, arXiv:1207.3346), the spatial distribution would be an additional strong test; in any case, it is of great interest to measure Sgr’s line-of-sight depth to establish the system’s axial ratios. Adopting $2r_{1/2}$ (axis A) to set a linear scale for the expected RR Lyrae spread along the line-of-sight semi-axis C , the extreme cases of a prolate system with $C = B$ versus an oblate system with $C = A$ equates to a total depth range variation of 2.0 versus 3.8 kpc — well within our ability to gauge with ~ 34 Sgr RR Lyrae, each with 2% ($= 0.6$ kpc) distance precision. Sgr would become the first dSph galaxy for which we could establish the true 3-D shape *and* orientation on the sky. The latter is set by the mean distance variation along the major axis including the ± 1 deg ring and ± 4 deg flanking fields. The LM10 N -body model specifically predicts a 2 kpc distance variation at ± 4 deg of Sgr center with the leading direction closer as a reflection of how debris is lost to the tails, whereas beyond ± 5 the distance trend actually reverses because debris then follows the shape of the Sgr orbit, which has increasing distance in the leading direction. In this way, the relative distance trend along the major axis is a very sensitive test of the specifics of the disruption model, and, in particular, the current Sgr mass, which drives the position of the inflection point.

- **Relative Placement of Sgr Globular Clusters:** It is now reasonably established that M54 and the Sgr core, while having the same photometric center, are distinct stellar populations (Siegel et al. 2007, ApJL, 667, L57) and structural entities (Majewski et al 2003, ApJ, 599, 1082) — i.e., Sgr has a nucleus independent of M54. It has been suggested that M54 began as an independent globular cluster that spiraled into Sgr center due to dynamical friction (Monaco et al. 2005, MNRAS, 356, 1396; Bellazzini et al. 2008, AJ, 136, 1147). However, a recent study using isochrone fitting to high precision, Hubble Space Telescope ACS photometry on the four Sgr core globular clusters as well as five locations on the Sgr core (Siegel et al. 2011, ApJ, 743, 20) reveals the surprising (3σ) result that M54 does *not* lie at the same *distance* as the Sgr core, but is actually closer by 2 kpc. The result has implications not only for the relation of M54 and the Sgr nucleus, but for the dark matter structure of the Sgr dSph, because a typically-cusped CDM profile would quickly (within a few Gyr) pull the cluster into the center (Bellazzini et al. 2008), whereas a cored profile would be more consistent with catching the system in the proposed 2 kpc-offset configuration. The Siegel et al. (2011) claim of a chance superposition of M54 2 kpc in front of Sgr can easily be checked with 2% (i.e., 0.6 kpc) distances on the proposed large samples of M54 and Sgr “ring” RR Lyrae. The signal would be clear as an offset between the $[Fe/H] = -1.55$ RR Lyrae of M54 and the $[Fe/H] = -1.2$ and -2.1 RR Lyrae of the Sgr core (Layden et al. 2000, AJ, 119, 1760; Cacciari et al. 2002, *Extragalactic Star Clusters*, 207, 168; Montiel & Mighell 2010). If, on the other hand, M54 was found, indeed, to lie at the same distance as Sgr, it would indicate errors in the adopted isochrones and, therefore, inferred properties (e.g., ages, He content,

detailed abundances) of the stellar populations in M54 and Sgr.

With precision isochrone fitting Siegel et al. (2011) found a 5 kpc distance spread in the Sgr core clusters. Measuring the relative placement of the other Sgr clusters to the main body is key to establishing whether they are still bound to Sgr, and can be checked by combining the proposed observations here with the RR Lyrae distances to Terzan 8 and Arp 2, which will also be observed in this program.

- **The Absolute Distance to Sagittarius:** The absolute distance to Sgr is still uncertain, with most original estimates clumping near 24 kpc (e.g., Ibata et al. 2004), but more recent measures steadily escalating from 26 to 30 kpc (e.g., Sollima et al. 2010, MNRAS, 406, 329; Monaco et al. 2004; Siegel et al. 2011; Layden et al. 2000). An accurate distance is crucial for understanding the strength of the Sgr/MW interaction, as well as serving as an anchor point to set the scale on any measurement of the MW potential. Spitzer observations of the RR Lyrae stars will resolve this issue at the 2% level, per star.

[Main body of Sgr, 23 lines of sight : 170 hr]

5.2 Probing Sagittarius’ Debris

We will target ~ 58 RR Lyrae stars distributed across 4 stretches of Sgr’s debris, two in the leading stream and two in the trailing stream. The density of RR Lyrae stars in the debris is sufficiently low that this will require 58 individual pointings and multiple visits. The total cost of this project will be ~ 250 hours. The RR Lyrae stars will be selected from stars associated with Sgr QUEST survey (Vivas et al. 2005), and from Stripe 82 of SDSS (Watkins et al. 2009). Both studies found significant clumps (82 and 55 stars respectively) with properties coincident with the “younger” (i.e. close in orbital phase to Sgr) leading (at ~ 60 kpc) and trailing (at ~ 25 kpc) portions of debris, in regions indicated by the red and blue points in the left-hand panel of Figure 3. The simulations suggest that there should also be less dominant but also less distant portions of the “older” debris within the same surveys. From the simulations we estimate a wrap of ~ 8 RR Lyrae stars of old trailing debris should lie along the same lines of sight as the young leading debris in the Vivas et al. (2005) sample, and ~ 25 RR Lyrae stars of old leading debris should lie along the same lines of sight as the old trailing debris in the Watkins et al. (2009) sample. Indeed, many closer RR Lyrae variables were found in both studies. We will use spectra and distance estimates to separate a sample of these closer stars that are consistent with our expectations for Sgr debris. Two key questions can be addressed with this sample.

- **Mapping the Path of Sgr Debris:** While the Sgr tidal arms have already been extensively mapped using carbon, M giant and MSTO stars, the distance estimates to these tracers have large (15-40%) random and (sometimes unknown) systematic uncertainties. Painstaking spectroscopic efforts (e.g. Chou et al. 2007, ApJ, 670, 346) have demonstrated the existence of metallicity spreads and gradients along the tidal arms, so that their 3-D orientation is presently subject to both large random uncertainties at each point and systematic uncertainties as a function of orbital phase. It is not yet clear how much these uncertainties have contributed to previous difficulties in modeling the system (Johnston et al. 2005, ApJ, 619, 800 ; Law et al. 2005, ApJ, 619, 807) or the surprising, unexpected shape and orientation of the MW dark halo inferred from the very latest attempts (LM10). The RR Lyrae measurements will (1) fix four orbital phase positions of the stream to a common distance scale to calibrate the stream distance-phase relationship for the other, more abundant tracers (M giants, MSTO stars), and (2) establish the line-of-sight depth of the debris,

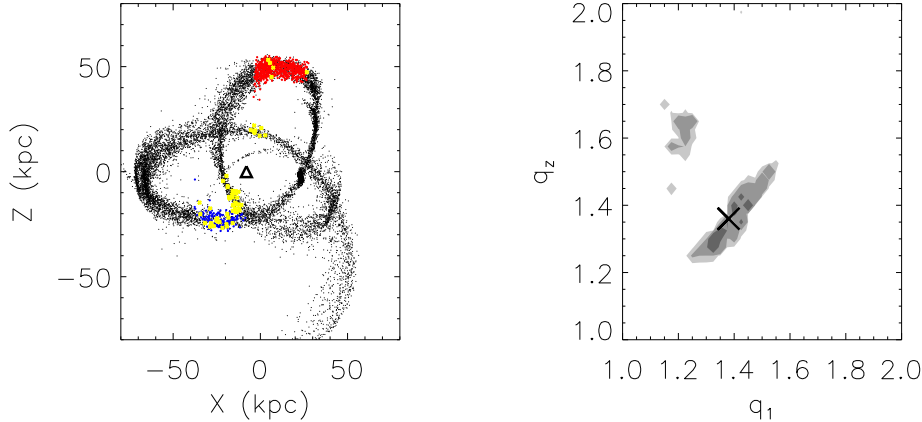


Figure 3 Left-hand plot shows the distribution of particles at the end-point of a simulation of the disruption of an object similar in mass and orbit to Sgr, with the triangle indicating the location of the Sun in this projection. The red and blue points represent regions where samples of RR Lyraes have been found by Vivas et al. (2005, AJ, 129, 189) and Watkins et al. (2009, MNRAS, 398, 1757), respectively. The yellow points represent our proposed RR Lyrae sample of ~ 58 stars. Right-hand panel illustrates the constraints the closest 53 stars can provide in the halo-shape-parameter plane (using a combination of Spitzer and Gaia data): q_1/q_2 and q_z/q_2 are the axis ratios of the dark matter potential in and perpendicular to the Galactic disk (ϕ , the orientation of q_1 in the disk-plane, was also allowed to vary). The cross indicates the parameter values in which the simulation was actually run. The grey scales show the one-, two- and three-sigma confidence levels, bootstrapped from the analysis of the 53 input stars.

which is directly correlated to the progenitor mass.

• **Constraining the Galactic Potential:** The promise of 2% accuracies for the RR Lyrae distances opens up an intriguing approach to measuring MW’s potential: The thickness of Sgr’s stream is actually greater than this uncertainty, so the measured position of each RR Lyrae relative to the stream is actually physically meaningful. Moreover, with Gaia’s final data release, there will be proper motion measurements of accuracies less than the intrinsic dispersion for much of the stream (e.g., corresponding to a tangential velocity accuracy of 10 km/s for an RR Lyrae at 35kpc) and ground-based radial velocities of few km/s accuracies can easily be added. Once the full phase-space positions of these stars are known there is no need to build a sophisticated model of the entire stream system to interpret the data. Instead, the knowledge that these stars were once part of Sgr allows them each to be exploited as individual potential measurers (as originally suggested by Johnston et al. 1999, ApJL, 512, L109) if the orbits of an RR Lyrae and Sgr are simultaneously integrated backwards in a potential that correctly models the MW, then their orbits must intersect at some point in the last few Gyrs; in an incorrect potential this will not happen.

Figure 3 (right panel) illustrates this idea for particles from the Sgr disruption N-body simulation chosen to represent our proposed RR Lyrae survey (yellow crosses in left panel). The 53 particles within 35 kpc of the Sun were “observed” with appropriate distance (assuming 2% accuracy), proper motion (assuming Gaia accuracies)¹ and radial velocity (assuming 5 km/s) errors. The “observed” phase-space positions were then integrated backwards in model

¹see <http://www.rssd.esa.int/index.php?project=GAIA>

potentials with axis ratios (q_1/q_2 and q_z/q_2) and orientation (ϕ) of the dark matter component systematically varied. Sgr's phase space coordinates (assumed to be exactly known, along with the distance to the Galactic center) were simultaneously integrated backwards in the same potentials, and the minimum normalized phase-space distance, D_{ps} , between Sgr and each particle recorded, where

$$D_{\text{ps}} = \left[\left(\frac{d}{r_{\text{tide}}} \right)^2 + \left(\frac{v}{v_{\text{esc}}} \right)^2 \right], \quad (1)$$

and d and v are the distance and speed separation between the star and Sgr respectively. The instantaneous tidal radius, $r_{\text{tide}} = R(m_{\text{sat}}/M_{\text{Gal}})^{1/3}$ and escape velocity, $v_{\text{esc}} = Gm_{\text{sat}}/r_{\text{tide}}$ for Sgr were calculated using a $2.5 \times 10^8 M_{\odot}$ mass for Sgr and estimating the mass of the Galaxy M_{Gal} enclosed within radius R directly from the assumed potential. The “best” potential parameters were those that minimized the average D_{ps} for all stars. Figure 3 (right panel) contours confidence levels for the recovered parameters (with a bold cross marking the true values used in the original simulation), with levels estimated by repeating the analysis using samples bootstrapped from our “observations”. The contours demonstrate the power of this combination of Spitzer and Gaia data: This small sample alone can broadly rule out significant areas of parameter space. Combining the constraints from these samples with the extensive ground-based data sets already available would allow quite clear measurements of the shape and depth of the Milky Way potential.

[48 RR Lyrae variables, 48 lines of sight, 262 hours]

6 Distances to Other Satellites

Gaia promises to revolutionize our understanding of the MW. For example, even at many tens of kpc, Gaia proper motion accuracies typically promise few percent measurements of the angular speed of satellites. However, Gaia parallaxes at these distances are much worse than 10%. Hence, exploiting RR Lyraes to find accurate distances to all MW satellites is of fundamental importance. Without these distances, the orbits for these objects will remain uncertain. As a starting point, we propose to find distances to three particularly interesting objects: Ursa Minor and Carina – both classical dwarf spheroidal galaxies; and Boötes – one of the more recently-discovered dwarfs whose nature is still under debate (Belokurov et al. 2006, ApJL, 647, L111). There are several topics that can be addressed with the combined Gaia and Spitzer measurements.

- **Interaction Induced Transformations of Galaxies:** It has long been recognized that there exists a strong density-morphology relationship within the Local Group in that dwarfs closer to either the MW or M31 are generally gas-poor, spherical and non-rotating, while those further away from the large galaxies are gas-rich, irregular and rotating (Grcevich & Putman, 2009, ApJ, 696, 385; Grebel et al. 2003, AJ, 125, 1926). Mayer et al. (2001, ApJL, 547, L123) proposed that this segregation is a signature of field irregulars being transformed by the combined effects of ram pressure stripping and tidal stirring as they are accreted by either of the larger galaxies to become spheroidal satellites. Subsequent simulations have described in some detail the stages of such transformations (Lokas et al. 2010). Indeed, all three of our target satellites appear to be undergoing transformation: Ursa Minor has an intriguing, double-core density structure with the main peak offset with respect to its outer isophotes (Bellazzini et al. 2002, AJ, 124, 3222); Carina exhibits tidal tails (Muñoz

et al. 2008, ApJ, 679, 346) and strong variations in star formation history, perhaps induced by compression of gas during pericentric passages (Monelli et al. 2003, AJ, 126, 218); and Bootes has a highly elongated morphology that is hard to reproduce through tidal effects on a purely spheroidal progenitor (Fellhauer et al, 2008, MNRAS, 385, 1095). Accurate orbits are essential to assess whether the depth and frequency of their pericentric passages are sufficient to take a dwarf irregular progenitor and reproduce these systems.

- **The Extent and Density of the Gaseous Halo of the Milky Way:** If the Mayer et al. (2001) picture is correct, and gas is lost from infalling dwarfs primarily due to ram pressure stripping, then each gas-poor satellite can provide an upper-limit to the Galactic halo gaseous density at the radius at which they orbit (see Grcevich & Putman 2009) However, since ram-pressure stripping is most effective for high-velocity encounters with dense gas, it is crucial to know the radius and speed at the pericenter of the orbit of each satellite in order to provide the tightest constraints.

- **The Formation and Evolution of the Galaxy’s Satellite System:** With the discovery of the ultra-faint dwarf galaxies, there has been renewed interest in the smallest galaxies we can see in the Universe (i.e., the satellites of the MW) because these galaxies probe the line between when a dark matter halo can and cannot form stars. Dark matter simulations of structure formation give us a clear picture about how the satellite dark matter subhalos might be accreted by and distributed about the MW (e.g., Diemand et al. 2007, ApJ, 667, 859), and suggest ways in which current orbits of subhalos might give us clues to their accretion time (e.g., Rocha et al. 2011, arXiv:1110.0464). It is of great interest to understand whether the subset of those dark matter subhalos containing baryons — i.e., the visible dwarf galaxy satellites of the MW — follow orbits that are similar to the entire dark matter subhalo population, or whether the necessary conditions for stars to form in a subhalo creates some differences. For example, Kunkel & Demers (1976, Roy. Green. Obs. Bull., 182, 241) first raised the idea that there might be physical connections between MW satellites when they noted curious alignments of dwarfs along great circles in the sky. Accurate measurements of satellite orbits could demonstrate whether these alignments are indeed a signature that dwarfs are biased by being born and infalling in groups.

[3 Milky Way satellites: 75 hr]

6.1 Calibrating the Tip of the Red Giant Branch (TRGB) Method

Finally, we note that with the determination of high-precision distances to the Large Magellanic Cloud, Ursa Minor and Carina we can now obtain three trigonometric-based zero points for the pure Population II distance scale by locking in the zero point of the TRGB Method using the RR Lyrae distances. Each of the above three systems have RR Lyrae variables co-existing spatially with their brighter distance indicators at the high end of the red giant branch. Quite independent of the Population I (Cepheid) distance scale we can now securely calibrate the TRGB method which can be then applied to all types of galaxies in which an old, halo population of RGB stars can be detected. The CRRP will have a calibration using Galactic globular clusters; SMASH will provide a complementary calibration within the Local Group. Application of the TRGB Method to significantly larger distances will take the pure Population II distance scale out to Type Ia supernovae and well into the pure Hubble flow. Having two independent paths to the Hubble constant will provide a much-needed check on the systematic uncertainty associated with this important cosmological parameter.

7 Technical Plan

The time-domain observing strategies adopted in this program build on experience gained by members of this team drawn from the successfully completed (Cycle 6: PI Freedman) Carnegie Hubble Program.

The Magellanic Cloud observations will provide 12 phase points per RR Lyrae variable. These will be obtained in four optimally-designed observing sessions per field. Each observing session will last for one hour, during which three, equally spaced phase points will be obtained. Four one-hour sessions scheduled within each 16 hour window will fully map the light curves with 12 relatively non-redundant data points. Template fitting of these well-sampled, low-amplitude ($\Delta[3.6] \sim 0.3$ mag) light curves will deliver mean magnitudes good to ± 0.015 mag. NB: OGLE IV will provide updated phases, and periods based contemporaneous ground-based VI observations being made by SMASH team members Udalski, Pietrzynski and Soszynski.

The Sagittarius fields will be observed at 12 epochs equally spaced over 16 hours. For the most distant of these fields (i.e. the furthest debris fields) we will observe continuously, with the observations broken into 12 AORs. We will observe every RR Lyrae target for at least 1 full cycle, enabling us to determine highly accurate distances ($\tilde{2}\%$) to each star. The fields will be positioned to maximize the number of RR Lyrae per pointing.

The Milky Way satellites are sufficiently distant that 16-hour sessions, which will be broken down into 12 individually integrated phase points, will be required for each target.

Team member Vicky Scowcroft has developed all of the software necessary for pipeline processing time-domain Spitzer/IRAC mosaics and pointed observations. This legacy software will be used for the SMASH program. As such we will be in a position to have calibrated light curves, mean magnitudes and distances to individual RR Lyrae stars and the systems in which they reside within days of us having received the preprocessed frames from the Spitzer Science Center.

To mitigate the potential effects of source confusion in our fields we will examine by eye the crowding of the individual RR Lyrae variables being targeted in each of the fields chosen in the first pass for their being the highest-density lines of sight at any given region in the satellite galaxies. We will use the V, I and K-band survey images available to us and adjust the field selections accordingly. The crowding at $2.2\ \mu\text{m}$ should be highly indicative of the crowding in the mid-IR.

8 Brief Team Resume

Our team is made up of a balanced blend of senior scientists, mid-career astronomers and younger members who have already established themselves as experts in their fields. Our team is deliberately small enough to be manageable, but still large enough to have expertise in each of the themes addressed in this proposal.

Steve Majewski, Kathryn Johnston and **David Nidever** are world leaders in the understanding of the structure, formation and evolution of our Galaxy and its largest satellites.

Nitya Kallivayalil has pioneered the use of HST in measuring the proper motions of the Magellanic Clouds.

Gurtina Besla is a leader in modeling proper motions and kinematics of the Magellanic Clouds.

David Law is actively involved in the study of the dynamics, stellar populations and mass distributions within Local group galaxies.

George Preston, Horace Smith & Giuseppe Bono have, quite literally, written the book on RR Lyrae stars, be it observational or theoretical.

Andrzej Udalski, Igor Soszynski and **Grzegorz Pietrzynski** are pioneers in time-domain surveys, and within the OGLE Project they are responsible for having discovered over 20,000 RR Lyrae stars in and around the Magellanic Clouds, and equal numbers in the Galactic bulge.

Gisella Clementini is a key member of the Gaia Team, and is their leading authority on variable stars, being especially cognizant of RR Lyrae variables.

Roeland van der Marel is the world authority on the 3D structure of the LMC and SMC.

Maria-Rosa Cioni is PI of the Vista Survey of the Magellanic System (VMC) and world leader in near-IR observations and studies of stellar populations in the Magellanic Clouds

Eric Persson is a widely respected instrumentalist and an authority on infrared detectors and photometry.

Ian Thompson has been observing globular clusters and Magellanic variable stars for decades, and recently determined the first high-precision mass estimate of an eclipsing Cepheid in the LMC.

Juna Kollmeier is a theorist whose interests include RR Lyrae variables and their application to Galactic structure and basic astrophysics. She has led the Carnegie RR Lyrae Survey (CARRS), a spectroscopic echelle survey undertaken at the duPont to obtain high-resolution spectra of over 1000 bright RR Lyrae which will reach completion in September 2012.

Vicky Scowcroft, Massimo Marengo, Andy Monson & Mark Seibert have extensive, demonstrable experience in observing with Spitzer in its warm mode, and in extracting high-precision, time-domain photometry from IRAC and WISE observations.

Wendy Freedman and **Barry Madore** have, for over thirty years now, been using variable stars in general, and IR techniques in particular, to refine the extragalactic distance scale and gauge the expansion rate of the Universe.

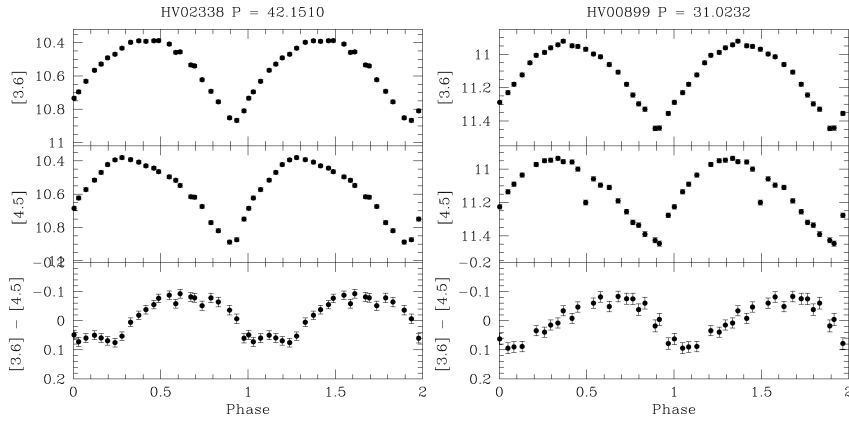


Figure 4 Two typical examples of the high-quality light curves that have been obtained by the CHP. These stars have the signal-to-noise as is being proposed for the Sagittarius RR Lyrae observations

9 Summary of the Carnegie Hubble Program

From the brightest Galactic variables to the faintest extragalactic Cepheids so far reduced, exquisite light curves are being generated by Spitzer. The project overall is on track to meet its proposed science objectives.

In the past three years the CHP has published six Spitzer/IRAC-based papers, presenting the mid-IR calibration of the Cepheid Period-Luminosity relation in the MW and in the LMC, and an early determination the extragalactic distance scale resulting in a value of the Hubble constant good to better than 3% has been made. Two additional papers are being refereed, and three more, discussing Spitzer-warm data for more galaxies, including the SMC will soon be submitted.

“The Carnegie Hubble Program” Freedman, W.L., et al. 2011, AJ, 142, 192

“The Carnegie Hubble Program: I. Mid-IR Light Curves and PL Relations for LMC Cepheids” Scowcroft, V., et al. 2011, ApJ, 743, 76

“The Carnegie Hubble Program: II. Galactic Cepheid Light Curves and PL Relations” Monson, A., et al., 2012, ApJ, accepted

“The Carnegie Hubble Program: A Mid-Infrared Calibration of the Hubble Constant” Freedman, W.L., et al., 2012, ApJ, accepted.

“The Carnegie Hubble Program: III. Mid-IR Distance to IC 1613” Scowcroft, et al., 2012, ApJ, submitted

“The Carnegie Hubble Program: IV. The Case of GR8” Scowcroft, et al., 2012, ApJ, submitted

“The Carnegie Hubble Program: V. Mid-IR Light Curves and PL Relations for SMC Cepheids” Scowcroft, V., et al. 2012, in preparation

“The Cepheid Period-Luminosity Relation at Mid-Infrared Wavelengths. I. First-Epoch LMC Data” Freedman, W.L., et al. 2008, ApJ, 679, 71

“The Cepheid Period-Luminosity Relation (The Leavitt Law) at Mid-Infrared Wavelengths. II. Second-Epoch LMC Data” Madore, B.F., et al. 2009, ApJ, 695, 988

“The Cepheid Period-Luminosity Relation (The Leavitt Law) at Mid-Infrared Wavelengths. III. Cepheids in NGC 6822” Madore, B.F., Rigby, J., Freedman, W.L., Persson, S.E., & Sturch, L. 2009, ApJ, 693, 936

“The Cepheid Period-Luminosity Relation (The Leavitt Law) at Mid-Infrared Wavelengths. IV. Cepheids in IC 1613” Freedman, W.L., Rigby, J., Madore, B.F., Persson, S.E., Sturch, L., & Mager, V. 2009, ApJ, 695, 996

Table 1. Observation Summary Table for Magellanic Cloud Targets

Target	RA J2000	DEC J2000	N_{point}	Frametime (s)	Est. flux (μ Jy)	Channels	Epochs	Fields
LMC1	05:32:32.25	-70:34:19.2	2×1	4×100	15 to 20	[3.6]	12	60
SMC1	00:37:07.89	-73:56:13.9	2×1	4×100	5 to 10	[3.6]	12	40

Table 2. Observation Summary Table for Sagittarius Targets

Target	RA J2000	DEC J2000	N_{point}	Frametime (s)	Est. flux (μ Jy)	Channels	Epochs	Fields
M54	18:55:03.0	-30:28:47	1×1	18×100	80 to 100	[3.6]	12	1
Arp 2	19:28:44.0	-30:21:20	1×1	18×100	80 to 100	[3.6]	12	1
Terzan 8	19:41:44.0	-33:59:58	1×1	18×100	80 to 100	[3.6]	12	1
SgrRing1	18:55:03.0	-29:28:47	1×1	18×100	80 to 100	[3.6]	12	1
SgrRing2	18:58:18.0	-29:46:21	1×1	18×100	80 to 100	[3.6]	12	1
SgrRing3	18:59:41.0	-30:28:47	1×1	18×100	80 to 100	[3.6]	12	1
SgrRing4	18:58:21.0	-31:11:13	1×1	18×100	80 to 100	[3.6]	12	1
SgrRing5	18:55:03.0	-31:28:47	1×1	18×100	80 to 100	[3.6]	12	1
SgrRing6	18:51:44.0	-31:11:13	1×1	18×100	80 to 100	[3.6]	12	1
SgrRing7	18:50:24.0	-30:28:47	1×1	18×100	80 to 100	[3.6]	12	1
SgrRing8	18:51:47.0	-29:46:21	1×1	18×100	80 to 100	[3.6]	12	1
SgrSide1	18:38:42.0	-29:34:27	1×1	18×100	80 to 100	[3.6]	12	6
SgrSide2	19:11:42.0	-31:23:07	1×1	18×100	80 to 100	[3.6]	12	6
SgrDebrisN	01:23:33.0	01:04:21	1×1	6×100	200 to 250	[3.6]	12	43
SgrDebrisF	14:34:43.64	01:13:08.8	1×1	45×100	20 to 25	[3.6]	12	8

10 Scheduling Profile

Both the SMC and LMC are largely in the “continuous viewing zone” accessible to Spitzer throughout the year. All of these observations should be easily scheduled.

The Sagittarius Dwarf Galaxy observations (and especially those associated with the tail) are widely separated across the sky and should impose no special requirements on when they are individually scheduled.

There are only three MW satellites and they can be scheduled whenever the SSC can slot them in.

11 Observation Summary Tables

Table 3. Observation Summary Table for Milky Way Satellites

Target	RA J2000	DEC J2000	N_{point}	Frametime (s)	Est. flux (μ Jy)	Channels	Epochs	Fields
UMi	15:09:08.49	67:13:21.4	1×1	45×100	20 to 25	[3.6]	12	1
Bootes	13:57:21.0	26:48:00.0	1×1	45×100	20 to 25	[3.6]	12	2
Carina	04:41:36.69	-50:57:58.3	1×1	60×100	5 to 10	[3.6]	12	1

12 Modification of the Proprietary Period

none requested

13 Summary of Duplicate Observations

Single observations of our some of our fields are undoubtedly in the Spitzer archive, but many of those frames are too shallow for our program and only constitute a sparse random sampling in space and time.

14 Summary of Scheduling Constraints/ToOs

Magellanic Clouds The Magellanic Cloud observations target individual RR Lyrae. We will optimise the fields to capture the greatest number of RR Lyrae per pointing. The observations are split into twelve epochs, grouped into 4 sets of 3 over 16 hours. The observations in the 3–epoch groups are chained, so that we are continuously observing the field for 1 hour. We then use follow-on constraints to repeat this sequence at $t = 5$, $t = 10$ and $t = 15$ hours from the start of the first group. This methodology ensures that we see the full pulsation cycle (which is typically a maximum of 16 hours) while still capturing the more rapid light variations. Representative AORs are included with the proposal. A summary of the observations is shown in Table 1.

Sagittarius Fields For the majority of the Sagittarius fields we use follow-on constraints to observe each field at regularly spaced intervals over 16 hours. For the more distant fields in the Sagittarius debris (labelled SgrDebrisF in Table 2) the exposure times become long enough that it is more efficient to use chained constraints to repeat the observation 12 times without moving the telescope. We want to ensure that we are observing each RR Lyrae for at least one unbroken cycle and chained observations are the only way to achieve this for the fainter targets. We have included representative AORs; the summary table is given in Table 2.

Milky Way Satellites As with the more distant Sgr Debris fields, the exposure times are long enough for the Milky Way satellites that the only way to make 12 observations over a single cycle is to use chained observations. Each chain takes around 20 hours, ensuring we will observe a full cycle of the longest period RR Lyrae stars (which can reach 1 day in extreme cases). There are no time constraints on when the chain can begin, except that it must be completable. This makes the scheduling of the observations very flexible. We have included representative AORs; the summary table is given in Table 3.